Proc. Natl. Acad. Sci. USA
Vol. 85, pp. 4133–4137, June 1988
Biochemistry

Structure of chloramphenicol acetyltransferase at 1.75-Å resolution

(antibiotic resistance/x-ray crystallography/coenzyme A/trimer)

ANDREW G. W. LESLIE*†, PETER C. E. MOODY*, AND WILLIAM V. SHAW‡

*Blackett Laboratory, Imperial College, London SW7 2BZ, United Kingdom; and ‡Department of Biochemistry, University of Leicester, Leicester LE1 7RH, United Kingdom

Communicated by E. R. Stadtman, January 13, 1988

ABSTRACT **Chloramphenicol acetyltransferase [acetyl-CoA:chloramphenicol O^3-acetyltransferase; EC 2.3.1.28] is the enzyme responsible for high-level bacterial resistance to the antibiotic chloramphenicol. It catalyzes the transfer of an acetyl group from acetyl CoA to the primary hydroxyl of chloramphenicol. The x-ray crystallographic structure of the type III variant enzyme from *Escherichia coli* has been determined and refined at 1.75-Å resolution. The enzyme is a trimer of identical subunits with a distinctive protein fold. Structure of the trimer is stabilized by a β-pleated sheet that extends from one subunit to the next. The active site is located at the subunit interface, and the binding sites for both chloramphenicol and CoA have been characterized. Substrate binding is unusual in that the two substrates approach the active site via clefts on opposite molecular "sides." A histidine residue previously implicated in catalysis is appropriately positioned to act as a general base catalyst in the reaction.**

Resistance to antibiotics in pathogenic bacteria is an increasingly common phenomenon, which has serious implications for clinical medicine. The resistance is frequently achieved by enzymatically catalyzed covalent modification of the drug. For chloramphenicol, inactivation is achieved by O-acetylation. Because the modified drug no longer binds to a bacterial ribosome, which is its normal site of action, the drug loses its effect as an antibiotic (1). The enzyme responsible for this acetylation is chloramphenicol acetyltransferase (CAT) (acetyl-CoA:chloramphenicol acetyltransferase; EC 2.3.1.28), which catalyzes transfer of an acetyl group from acetyl CoA to the primary hydroxyl (C-3) of chloramphenicol (Cm) (2–4).

$$\text{Cm} + \text{acetyl CoA} \rightleftharpoons \text{acetyl-Cm} + \text{CoA-SH}$$

The CAT gene is commonly, but not exclusively, plasmid-borne in natural isolates and has been found to be a component of plasmids conferring multiple drug resistance, especially in Gram-negative bacteria and the *Enterobacteriaceae*, in particular (5). Amino acid sequences of several variants of CAT from both Gram-positive and Gram-negative bacteria have been determined (6–11). All known variants have similar subunit molecular weights ($M_r \approx 25{,}000$) and are highly homologous, indicating similar tertiary structure. This conclusion had been inferred from earlier studies of hybrids formed *in vivo* and *in vitro* between naturally occurring variants (12, 13). Although the hybridization results were originally interpreted in terms of a tetrameric structure for CAT, crystallographic work and more recent hydrodynamic results (14) clearly show that CAT is a trimer, a relatively unusual oligomeric symmetry for a soluble enzyme. Of known variants of CAT, those currently best characterized are the type I protein, typified by the CAT encoded by transposon Tn*9* and in wide use as a tool for studying gene expression in eukaryotic systems (15), and the type III variant, which has been studied by kinetic and chemical methods (16, 17) and which is currently the only variant to yield crystals suitable for x-ray diffraction studies (18).

We report here the three-dimensional structures of two binary complexes of CAT, one with the substrate chloramphenicol bound and the second with bound CoA (a product of the forward reaction and substrate for the reverse reaction).

Structure Determination

Crystals of the binary complex of the enzyme with bound chloramphenicol were obtained by microdialysis of protein (5 mg/ml) in 10 mM Mes, pH 6.3, against 2% (vol/vol) 2-methyl-2,4-pentandiol/10 mM Mes, pH 6.3/1 mM chloramphenicol/0.5 mM hexaminecobalt(III) chloride (18). The cobalt salt was essential for successful crystallization. The space group is *R*32 (a = 74.5 Å, α = 92.5°), with a monomer in the crystallographic asymmetric unit. X-ray data were collected photographically by use of an Arndt–Wonacott oscillation camera and were processed with the MOSFLM program. The 1.75-Å-resolution native data set was recorded at the synchrotron radiation source at Daresbury, U.K., with radiation of wavelength 0.90 Å. All other data sets were obtained with a rotating anode x-ray source and CuK$\bar{\alpha}$ radiation. Data were collected from native crystals and five isomorphous derivatives. The structure was solved using conventional multiple isomorphous replacement techniques at 2.7-Å resolution (Table 1). The polypeptide backbone was traced initially from a "minimap" (scale, 4 Å = 1 cm), and this solution was readily confirmed with the aid of the latest version of the interactive graphics program FRODO (20), which incorporates the chain-tracing algorithm of Greer (21). A molecular model was built from the known-amino acid sequence with the use of the "fragment fitting" feature (22) of the same version of FRODO. This procedure greatly facilitated construction of a molecular model with acceptable stereochemistry, particularly in those regions (predominantly extended loops or turns) where electron density was poorly defined. The model was refined by use of a modified version of the Hendrickson–Konnert restrained refinement program (23), in which structure factors and their derivatives are calculated using fast-Fourier-transform algorithms (24, 25). During refinement, resolution of the x-ray data was extended in steps from 2.7 Å to 1.75 Å. The final model, which includes bound chloramphenicol and 135 solvent molecules, has acceptable stereochemistry (Table 2) and a crystallographic *R* factor of 19.0% for all reflections between 6-Å and 1.75-Å resolution.

Crystals of the enzyme with bound CoA were obtained by microdialysis of protein (5 mg/ml) against 18% 2-methyl-2,4-pentandiol/10 mM Mes, pH 6.3/0.7 mM CoA/5 mM β-mercaptoethanol/0.5 mM hexaminecobalt(III) chloride.

The publication costs of this article were defrayed in part by page charge payment. This article must therefore be hereby marked "*advertisement*" in accordance with 18 U.S.C. §1734 solely to indicate this fact.

Abbreviation: CAT, chloramphenicol acetyltransferase.

†To whom reprint requests should be addressed.

Table 1. Data collection and isomorphous derivative statistics

Data set	Resolution, Å	Multiplicity*	R_m†, %	R_d‡, %	Number of heavy atom sites	Phasing§ power	R_C¶, %
CAT–CM	2.5	4.2	5.9				
CAT–CM	1.75	3.5	5.8				
$KAu(CN)_2$ (5 mM)	2.7	3.5	4.4	17.0	3	2.92	51.3
$KAu(CN)_2$ (2 mM)	2.7	3.6	4.4	13.2	3	2.34	58.1
PICM	2.7	2.4	4.5	10.1	2	1.32	61.2
PHMB	2.7	2.2	4.6	12.1	2	1.38	65.6
K_2PtCl_4	4.0	2.1	7.0	13.8	2	0.88	82.6
CAT–CoA	2.4	2.8	7.0	14.8			

CM, chloramphenicol; PICM, *p*-iodophenyl derivative of chloramphenicol; PHMB, *p*-hydroxymercuribenzoate. Heavy-atom variables were refined using a phase-refinement program (19), and multiple isomorphous replacement phases were calculated to 2.7-Å resolution with an overall figure of merit (which is a measure of the quality of the phases) of 0.72.
*Multiplicity equals total no. of observations/no. of independent reflections.

†Merging R factor, $R_m = \frac{\Sigma\Sigma|I(h)_j - \langle I(h)\rangle|}{\Sigma\Sigma\, I(h)_j}$, where $I(h)$ is the measured diffraction intensity, and the summation includes all observations.

‡Derivative R factor, $R_d = \frac{\Sigma|F_{nat} - F_{deriv}|}{\Sigma\ F_{nat}}$ where F_{nat} and F_{deriv} are the native (CAT–chloramphenicol) and derivative-structure factor amplitudes.

§Phasing power $= \frac{\text{rms heavy-atom structure factor}}{\text{rms lack of closure}}$.

¶Cullis R factor, $R_C = \frac{\Sigma|FPH_{calc} - FPH_{obs}|}{\Sigma\ FPH_{obs}}$ for centric terms only, where FPH is the derivative-structure factor.

These crystals are isomorphous with those of the enzyme with bound chloramphenicol. X-ray data were collected to 2.4-Å resolution (Table 1). A difference electron-density map between the two binary complexes using model phases clearly revealed the position of bound CoA. The structure of the enzyme–CoA complex was refined at 2.4-Å resolution, using the refined structure of the enzyme–chloramphenicol complex as a starting model. The final refined structure has a crystallographic R factor of 20.4% for all data between 10 Å and 2.4 Å and good stereochemistry (Table 2).

General Description of the Structure

The dominant feature of the structure of the monomer, shown schematically in Fig. 1, is a six-stranded predominantly antiparallel β-pleated sheet, which displays the characteristic left-handed twist. Packed against the ends and one face of the sheet are five α-helices, accounting for 28% of the 213 residues. This arrangement of α-helices and β-sheet is not uncommon in protein structures and has been described as an "open-face sandwich" (26), but the precise folding pattern seen in CAT shows no direct similarity to any known protein structure. Three monomers associate to form a compact disc-shaped trimer (Fig. 2) ≈ 65 Å in diameter and 40 Å thick. In the trimer the extended strand β_E, which is somewhat isolated in the structure of the monomer, forms an extension to the six-stranded sheet of an adjacent subunit, resulting in a seven-stranded sheet that spans the subunit interface. Similar extensions of a β-sheet on formation of an oligomer from its constituent monomers have been seen in other structures (prealbumin, concanavalin A, and insulin), but extension by a single strand is less common. This feature may help account for the observed stability of the oligomeric enzyme form (5).

Table 2. Deviations from ideal geometry of the refined CAT models

	σ_i*	CAT–CM complex rms deviation	CAT–CoA complex rms deviation
Distance, Å			
Bond	0.02	0.02	0.02
Angle	0.03	0.04	0.04
Intraplanar	0.05	0.06	0.06
Planar group	0.02	0.02	0.02
Chiral center	0.15	0.18	0.16
Torsion angle, °			
Staggered (χ_1 aliphatic)	15.0	13.9	16.0
Transverse (χ_2 aromatic)	20.0	27.1	27.0
Nonbonded contact, Å			
Single torsion	0.20	0.16	0.17
Multiple torsion	0.20	0.22	0.18
Thermal factor, Å²			
Main-chain bond	2.0 (1.5)	4.2	4.3
Main-chain angle	3.0 (2.5)	5.2	6.1
Side-chain bond	3.0 (2.5)	6.2	7.1
Side-chain angle	4.0 (3.5)	7.8	8.4

*σ_i (where i = input) values determine relative weights of each restraint in the refinement. When different σ values were used to refine the two structures, values in parentheses are for the CAT–CoA refinement.

The conformation of the enzyme is essentially identical in the two binary complexes. The independently refined structures can be superimposed to give an rms deviation in atomic coordinates of 0.3 Å for all protein atoms (0.15 Å for main-chain atoms alone), which is comparable to the accuracy of the coordinates. The largest main-chain movement is only 0.34 Å for Lys-54, which is located at the entrance to the CoA-binding pocket.

The Chloramphenicol-Binding Site

The subunits of CAT associate to produce a well-defined pocket at the subunit interface that accommodates the chloramphenicol molecule and several ordered water molecules (Figs. 2 and 3). The residues lining the pocket are predominantly hydrophobic, and there are only two direct hydrogen bonds between the substrate and the enzyme, with an additional hydrogen bond via a bridging water molecule. Only five of these residues are strictly conserved among all known CAT sequences, but the observed substitutions are always conservative. The conformation of chloramphenicol is very similar to that seen in the single-crystal structure (27)

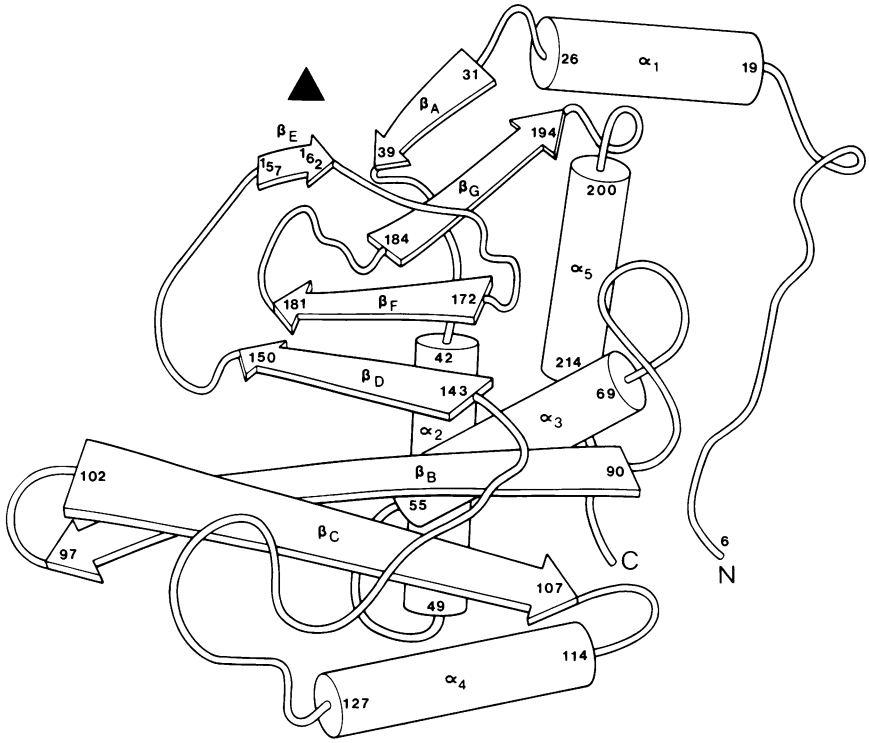

FIG. 1. Schematic of the chain fold of a single CAT subunit viewed down the trimer axis (indicated by arrowhead). Amino acid numbering scheme is based on alignment of type III, type I, and type C variants of CAT. Our numbering is related to the type III linear sequence by adding 5 to residues 1–74 and 6 to residues 75–213 of the linear sequence.

(rms deviation in coordinates, 0.5 Å) and consistent with that postulated for chloramphenicol in solution on the basis of NMR studies and potential energy calculations (28). The major difference is that the primary (C-3) hydroxyl of enzyme-bound chloramphenicol (the acetyl acceptor in the forward reaction) adopts an alternative staggered conformation to that seen in the crystal structure of the antibiotic. As a consequence, the primary hydroxyl is correctly placed to form a hydrogen bond with the ring nitrogen (N-3) of the active site histidine (His-195) (Fig. 3). The nitro group and one of the two chlorines point out of the pocket and are solvent-accessible, consistent with results of kinetic studies of CAT that demonstrated acetyl acceptor activity with chloramphenicol analogues having substitutions for the *p*-nitro and *N*-dichloroacetyl moieties (5).

The CoA-Binding Site

When chloramphenicol is bound, access to the active site is completely blocked from the top of the enzyme as viewed in Fig. 2. This suggests that the second substrate (acetyl CoA) must approach the active site from a different direction because no kinetic evidence favors the view that ordered binding of the substrates is obligatory (16). In the refined structure of the CAT–chloramphenicol complex a remarkable tunnel leads from the active-site histidine out to the lower surface of the enzyme (as viewed in Fig. 2). Apart from a short spur, this tunnel is approximately cylindrical in shape, 3–4 Å in diameter and 12 Å in length, and is occupied by six ordered solvent molecules. Modeling studies suggested that the tunnel could readily accommodate the pantetheine arm of CoA in an extended conformation, placing the adenosine and phosphate moeities on the external surface of the CAT molecule. After completion of data collection from crystals of the CAT–CoA complex, a difference electron-density map between the two binary complexes immediately confirmed the proposed binding site.

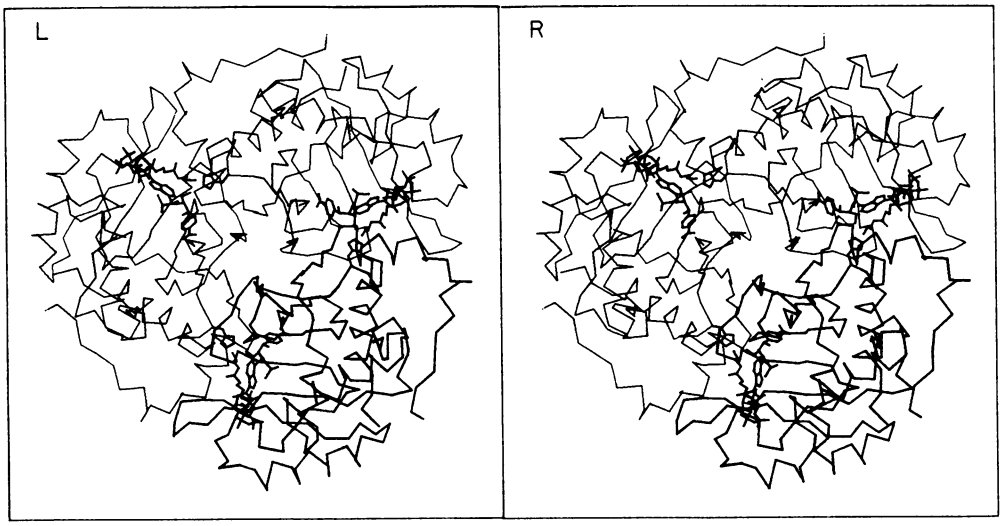

FIG. 2. Stereoview of C_α backbone of the CAT trimer viewed down the trimer axis. One subunit has been drawn in boldface to clarify the position of the subunit interface. Chloramphenicol, CoA, and the active site His-195 are also shown. The chemical structure of chloramphenicol appears in Fig. 5.

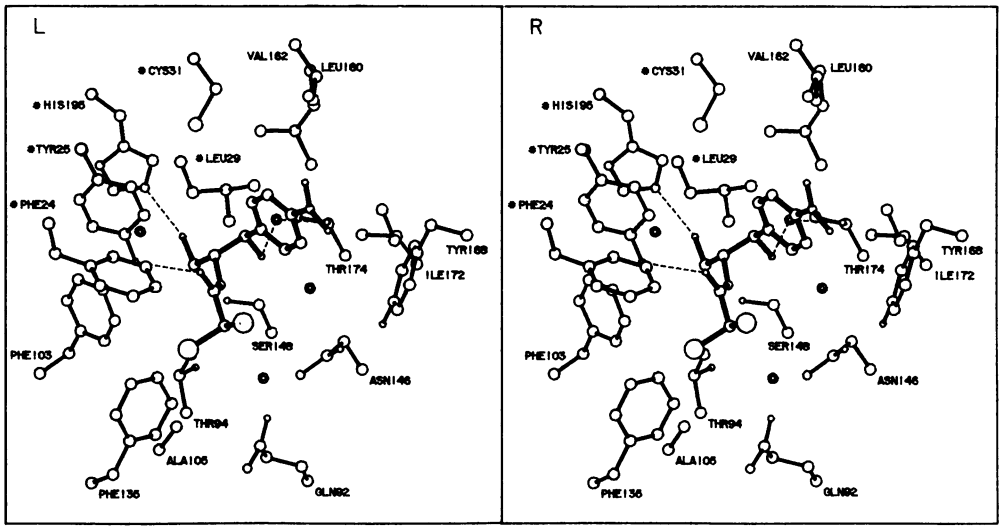

FIG. 3. Stereoview of the chloramphenicol-binding pocket, showing the conformation of enzyme-bound chloramphenicol (boldface), active-site histidine (His-195), and residues involved in binding-site formation. ---, Predicted hydrogen bonds; ○, ordered solvent molecules.

Location of bound CoA is shown in Fig. 2, and a more detailed picture of the residues involved in binding is given in Fig. 4. Hydrophobic interactions clearly play an important role in CoA binding. The pantetheine arm is almost fully extended and runs between the carboxyl ends of strands β_B and β_D of the β-pleated sheet. Both main-chain and side-chain atoms from residues on these two strands together with the side chains of Tyr-56, Phe-96, and Phe-103 contribute to the formation of the tunnel-like binding pocket. In contrast to the pantetheine arm, the adenosine 5′-diphosphate component adopts a folded conformation that brings the adenine ring into van der Waals contact with the dimethyl group of the pantetheine arm. The ribose conformation is $C^{2'}$-*endo*, and the glycosidic torsion angle is *anti*. The adenine ring binds in a hydrophobic pocket formed by the side chains of Phe-55, Pro-151, and Tyr-178 and forms hydrogen bonds with the main-chain amide of Tyr-178 and the carbonyl oxygen of Ala-176. The only other direct hydrogen bonds between CoA and the enzyme are between the amide of the β-mercapto ethylamine component of CoA and the main-chain carbonyl oxygen of Ala-149 and interactions involving the CoA thiol group, although there are additional hydrogen bonds via bridging water molecules (Fig. 4). Surprisingly, there are no basic side chains interacting directly with any of the three phosphate groups, nor are any of the phosphate groups in a position that would lead to a favorable interaction with the dipole moment of an α-helix, as is commonly seen in the structures of dinucleotide-binding proteins (29).

In some respects the mode of binding of CoA is rather similar to that seen in citrate synthase (30): the pantetheine arm is completely shielded from bulk solvent, while the phosphate groups are located at the enzyme surface. However, the conformation of CoA is quite different in the two structures. When bound to citrate synthase, the molecule adopts a much more compact folded conformation, characterized by two internal hydrogen bonds (one via a bridging water molecule). Details of the interactions are also rather different. The adenine ring forms hydrogen bonds to main-chain atoms in both structures, but in CAT there is no obvious counterpart to the "adenine recognition loop" described for citrate synthase. In addition, the phosphate groups are coordinated by three arginine residues in citrate synthase, whereas no similar feature exists in CAT. In view of the conformational flexibility of CoA, lack of similarity between the binding sites in these two enzymes is, perhaps, not surprising.

Interestingly, in the absence of bound chloramphenicol, the acetyl-CoA tunnel and the chloramphenicol-binding cleft

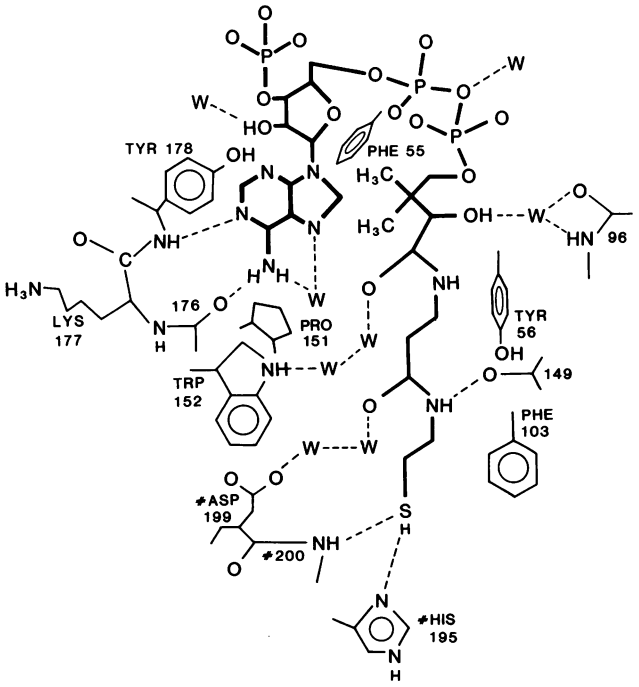

FIG. 4. Schematic of the CoA-binding pocket. ---, Predicted hydrogen bonds; W, ordered solvent molecules. Residue names preceded by # belong to an adjacent subunit.

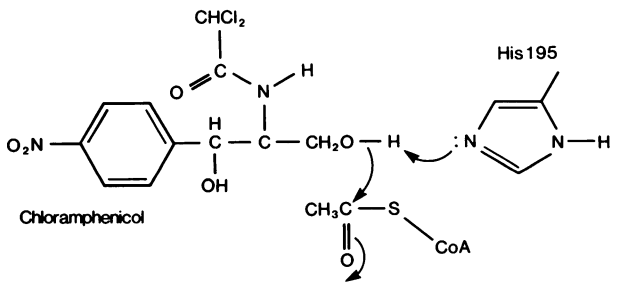

FIG. 5. Proposed role of the active-site histidine (His-195) as a general base catalyst in the acetyl-transfer reaction.

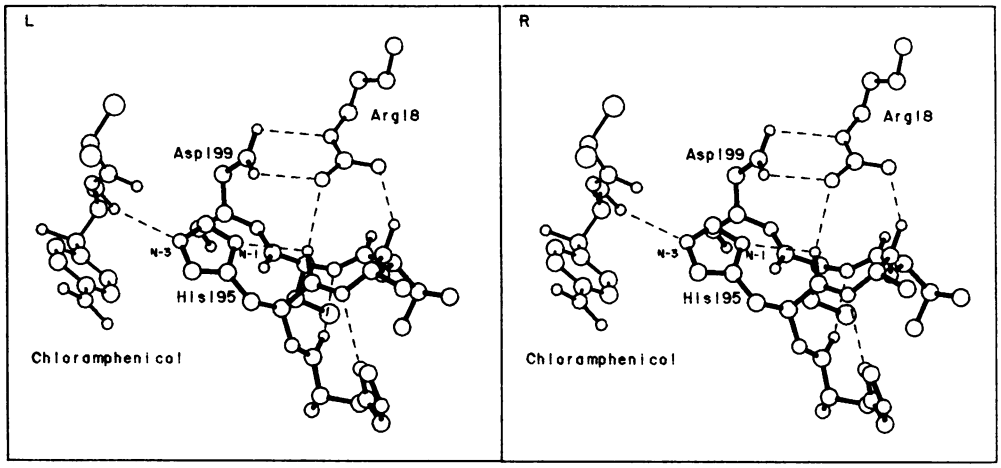

FIG. 6. Stereoview of a hydrogen-bonding scheme for residues near the active site.

combine to form a continuous solvent-accessible pathway ≈25 Å in length—extending from one side of the molecule to the other, a feature rarely seen in protein structures.

The Active Site

Chemical modification experiments (17) and site-directed mutagenesis (31) have indicated that His-195 plays an essential role in catalysis and also implicate the carboxyl group of Asp-199. Steady-state kinetic studies (16) suggest a ternary complex (sequential) rather than a ping-pong mechanism, arguing for a general base role for His-195, with deprotonation of the C-3 hydroxyl of chloramphenicol and nucleophilic attack on the carbonyl of the thio ester of acetyl CoA (Fig. 5). The present structure reveals a network of hydrogen bonds in the active site (Fig. 6). Asp-199 (conserved in known sequences) is involved in a salt-bridge to the side chain of Arg-18 (also conserved), which, in turn, is within hydrogen-bonding distance of the main-chain carbonyl oxygens of residues 195 and 196. The side chain of the active-site His-195 adopts an unusual conformation ($\chi_1 = -146$, $\chi_2 = -29$), which allows formation of a hydrogen bond between the imidazole nitrogen N-1 and the carbonyl oxygen of the same residue. (A search of the Brookhaven data base revealed no other example of this type of interaction.) The imidazole ring is also in van der Waals contact with the benzene ring of Tyr-25 (Fig. 3), and this interaction may help stabilize the side-chain orientation. The unusual conformation of His-195 would allow the imidazole N-3 nitrogen to abstract a proton from the primary hydroxyl of chloramphenicol, consistent with the mechanism outlined above (Fig. 5).

When the CoA coordinates from the enzyme–CoA complex are transposed into the refined enzyme–chloramphenicol model, the thiol group is positioned at distances of 3.3 Å and 2.8 Å from the N-3 nitrogen of His-195 and the primary hydroxyl of chloramphenicol, respectively. Thus, no major structural rearrangement is needed to bring the components into proximity for catalysis to proceed, although further work is necessary to grasp the details of this mechanism. Site-directed mutagenesis of residues in the active site (31) should help clarify the role of individual amino acids in catalysis.

We thank David M. Blow, Peter Brick, and Alan J. Wonacott for discussions and encouragement and Philip R. Evans, Eleanor Dodson, and Alwyn Jones for computer programs. This work has been supported by the Medical Research Council through project grants and a Medical Research Council Senior Fellowship to A.G.W.L.

1. Gale, E. F., Cundliffe, E., Reynolds, P. E., Richmond, M. H. & Waring, M. J. (1981) *The Molecular Basis of Antibiotic Action* (Wiley, London), 2nd Ed., pp. 460–468.
2. Shaw, W. V. (1967) *J. Biol. Chem.* **242,** 687–693.
3. Suzuki, Y. & Okamoto, S. (1967) *J. Biol. Chem.* **242,** 4722–4730.
4. Shaw, W. V. & Unowsky, J. (1968) *J. Bacteriol.* **95,** 1976–1978.
5. Shaw, W. V. (1983) *CRC Crit. Rev. Biochem.* **14,** 1–46.
6. Alton, N. K. & Vapnek, D. (1979) *Nature (London)* **282,** 864–869.
7. Shaw, W. V., Packman, L. C., Burleigh, B. D., Dell, A., Morris, H. R. & Hartley, B. S. (1979) *Nature (London)* **282,** 870–872.
8. Horinouchi, S. & Weisblum, B. (1982) *J. Bacteriol.* **150,** 815–825.
9. Shaw, W. V., Brenner, D. G., Le Grice, S. F. J., Skinner, S. E. & Hawkins, A. R. (1985) *FEBS Lett.* **179,** 101–106.
10. Charles, I. G., Keyte, J. W. & Shaw, W. V. (1985) *J. Bacteriol.* **164,** 123–129.
11. Murray, I. A., Hawkins, A. R., Keyte, J. W. & Shaw, W. V. (1988) *Biochem. J.* **252,** in press.
12. Sands, L. C. & Shaw, W. V. (1973) *Antimicrob. Agents Chemother.* **3,** 299–305.
13. Packman, L. C. & Shaw, W. V. (1981) *Biochem. J.* **193,** 541–552.
14. Harding, S. E., Shaw, W. V. & Rowe, A. J. (1987) *Biochem. Soc. Trans.* **15,** 513.
15. Gorman, C. M., Moffat, L. F. & Howard, B. H. (1982) *Mol. Cell. Biol.* **2,** 1044–1051.
16. Kleanthous, C. & Shaw, W. V. (1984) *Biochem. J.* **223,** 211–220.
17. Kleanthous, C., Cullis, P. M. & Shaw, W. V. (1985) *Biochemistry* **24,** 5307–5313.
18. Leslie, A. G. W., Liddell, J. M. & Shaw, W. V. (1986) *J. Mol. Biol.* **188,** 283–285.
19. Bricogne, G. (1982) in *Computational Crystallography*, ed. Sayre, D. (Clarendon, Oxford, U.K.), pp. 223–230.
20. Jones, T. A. (1978) *J. Appl. Crystallogr.* **11,** 268–272.
21. Greer, J. (1985) *Methods Enzymol.* **115,** 206–224.
22. Jones, T. A. & Thirup, S. (1986) *EMBO J.* **5,** 819–822.
23. Hendrickson, W. A. & Konnert, J. H. (1980) in *Computing in Crystallography*, eds. Diamond, R., Ramaseshan, S. & Venkatesan, K. (Natl. Acad. Sci. India, Bangalore, India), pp. 13.01–13.23.
24. Agarwal, R. C. (1978) *Acta Crystallogr. Sect. A* **34,** 791–809.
25. Isaacs, N. (1982) in *Computational Crystallography*, ed. Sayre, D. (Clarendon, Oxford, U.K.), pp. 398–408.
26. Richardson, J. S. (1981) *Adv. Protein Chem.* **34,** 167–339.
27. Chatterjee, C., Dattagupta, J. K., Saha, N. N., Saenger, W. & Muller, K. (1979) *J. Cryst. Mol. Struct.* **9,** 295–300.
28. Bustard, T. M., Egan, R. S. & Perun, T. J. (1973) *Tetrahedron* **29,** 1961–1967.
29. Wierenga, R. K., De Maeyer, M. C. H. & Hol, W. G. J. (1985) *Biochemistry* **24,** 1346–1357.
30. Remington, S., Wiegand, G. & Huber, R. (1982) *J. Mol. Biol.* **158,** 111–152.
31. Murray, I. A., Lewendon, A., Kleanthous, C. & Shaw, W. V. (1986) *Biochem. Soc. Trans.* **14,** 1227–1228.